LETTER

High-conductance contacts to functionalized molecular platforms physisorbed on Au(1 1 1)

View the article online for updates and enhancements.

IOP ebooks™

Bringing you innovative digital publishing with leading voices to create your essential collection of books in STEM research.

Start exploring the collection - download the first chapter of every title for free.

Letter

High-conductance contacts to functionalized molecular platforms physisorbed on Au(1 1 1)

Torben Jasper-Tönnies[1] ⓘ**, Aran Garcia-Lekue**[2,3] ⓘ**, Thomas Frederiksen**[2,3] ⓘ**, Sandra Ulrich**[4]**, Rainer Herges**[4] ⓘ **and Richard Berndt**[1] ⓘ

[1] Institut für Experimentelle und Angewandte Physik, Christian-Albrechts-Universität, 24098 Kiel, Germany
[2] Donostia International Physics Center, DIPC, Paseo Manuel de Lardizabal 4, E-20018 Donostia-San Sebastián, Spain
[3] IKERBASQUE, Basque Foundation for Science, E-48013 Bilbao, Spain
[4] Otto-Diels-Institut für Organische Chemie, Christian-Albrechts-Universität, 24098 Kiel, Germany

E-mail: jasper-toennies@physik.uni-kiel.de

CrossMark

Abstract
The conductances of molecules physisorbed to Au(1 1 1) via an extended π system are probed with the tip of a low-temperature scanning tunneling microscope to maximize the control of the junction geometry. Inert hydrogen, methyl, and reactive propynyl subunits were attached to the platform and stand upright. Because of their different reactivities, either non-bonding (hydrogen and methyl) or bonding (propynyl) tip-molecule contacts are formed. The conductances exhibit little scatter between different experimental runs on different molecules, display distinct evolutions with the tip-subunit distance, and reach contact values of 0.003–0.05 G_0. For equal tip-platform distances the contact conductance of the inert methyl is close to that of the reactive propynyl. Under further compression, the inert species, hydrogen and methyl, are found to be better conductors. This shows that the current flow is not directly correlated with the chemical interaction. Atomistic calculations for the methyl case reproduce the conductance evolution and reveal the role of the junction geometry, forces and orbital symmetries at the tip-molecule interface. The current flow is controlled by orbital symmetries at the electrode interfaces rather than by the energy alignment of the molecular orbitals and electrode states. Functionalized molecular platforms thus open new ways to control and engineer electron conduction through metal-molecule interfaces at the atomic level.

Keywords: conductance, charge transport, electronic structure, scanning tunneling microscopy, first-principle calculations, molecule-metal junction

S Supplementary material for this article is available online

(Some figures may appear in colour only in the online journal)

The transport of electrons through molecule-metal junctions is relevant for processes in many branches of science and crucial for potential applications in electric engineering [1–6]. However, understanding and tailoring the charge transport through a molecule-metal junctions is a major challenge, because it drastically depends on geometric and electronic details of the molecule-metal interfaces [1–5, 7–15]. Chemical anchor groups comprising a molecular subunit

or a single atom attached to the molecule of interest have been used to achieve well-defined interfaces [2–5, 8, 9, 16, 17]. In particular, reactive anchor groups that chemisorb to metal electrodes have been a focus of interest, because they are expected to provide strong forces that stabilize a desired molecule-electrode geometry [4, 5, 9, 16, 17]. However, bond formation tends to induce significant electronic changes of the electrode-molecule complex and renders difficult the design of a molecule that will deliver specific transport properties [2, 3, 8–10, 17].

Here, we explore the transport properties of a class of molecules that rely on a different anchoring scheme. It is designed to leave the properties of the functional molecular subunit almost unaffected by avoiding strong hybridization of the molecular states with those of the electrode. This is achieved by using a platform that binds to metal substrates via physisorption. Functional subunits are attached to its center and stand upright. Like other platform molecules it can be used to achieve decoupling from neighbor molecules [18]. In contrast to the triazatriangulenium (TATA) platform [19–21], the trioxatriangulenium (TOTA) we use here may be sublimated intact, and thus enables systematic investigations in ultrahigh vacuum. The extended π system of the platform provides a high-conductance contact to the substrate [22], as expected (see, e.g. [5, 12, 23]). To the best of our knowledge, the only *physisorbed* multidentate molecular anchors that enabled stable contacts to metal electrodes so far are fullerenes, pyrene and benzene [5, 12, 16, 24, 25].

We investigated the conductance of platform-based molecules by controllably contacting them with the atomically sharp tip of a scanning tunneling microscope (STM). The geometries before contact formation were monitored by STM imaging. Contacts to inert and rigid functional units, methyl and hydrogen, turned out to exhibit similar conductances as a reactive propynyl wire that covalently binds to the STM tip[5][26]. Atomistic transport calculations, however, show that different orbitals carry the current in these cases. Orbital symmetries are shown to affect the conductance as previously reported for small molecules (see, e.g. [27, 28]). In addition, the forces acting across the tip-molecule-surface junction affect the geometry and the conductance-versus-distance data.

Experimental results

Metal-molecule junctions

TOTA (figure 1(a)) was used as a platform. The bare platform and TOTA functionalized with hydrogen, methyl and propynyl (H-TOTA, Me-TOTA and P-TOTA, figures 1(b)–(d)) were sublimated onto Au(1 1 1) surfaces at ambient temperature and studied with STM at 4.6 K (see Methods). Single molecules appear as triangular protrusions in STM images (figures 1(e)–(h)). The attached methyl and propynyl moieties are imaged as circular protrusions at the center of the platforms (figures 1(g)

---

[5] We use the term bond or bonded according the AIM (atoms in molecules) definition [26]. This definition implies that there is significant electron density between two atoms that are bonded to each other.

and (h)). The H atom in H-TOTA (figure 1(f)) is not resolved, as expected (see, e.g. [29, 30]). The molecules were contacted at their center with Au tips, whose apex orbital, close to the Fermi level, may be modelled as an *s* orbital. The measurements were conducted at molecules in small clusters to reduce lateral movements. Results from the reactive P-TOTA molecules have been discussed in detail [22] and are used here for comparison.

A related platform, TATA, was previously investigated in an electrochemical environment [20]. Those experiments did not allow for the degree of control available in the present work. Nonetheless, conductances similar to those of thiols were found for junctions comprising one or a few ten molecules. In contrast to TATA, we found TOTA derivatives to be robust towards sublimation. Moreover, their conductances are more than two orders of magnitude higher, i.e. TOTA is more suitable as a high-conductance anchor group.

Conductances versus electrode position

Figure 1(i) displays the conductances G measured while the electrode, i.e. STM tip, was moved closer to the center of a molecule from the initial tunneling conditions ($V = 100$ mV, $I = 30$ pA). The position z of the tip is referenced to the point of contact that was observed with the same tip on a bare fcc area of the Au(1 1 1) substrate (yellow curve). Before contact ($z > 0$ Å), the Au contact curve (yellow) exhibits an exponential variation (apparent tunneling barrier height: ≈ 4 eV) that reflects the size of vacuum tunneling gap. At $z = 0$ Å it abruptly rises to 1 G_0. This effect reflects (i) the formation of a bond to the Au(1 1 1) surface and (ii) a related elastic elongation of the Au tip [31, 32]. After bond formation ($z < 0$ Å), the conductance varies only weakly.

The conductance curve of the bare TOTA platform (black curve, figure 1(i)) serves as a reference. In the tunneling regime ($z < 2.2$ Å), the bare platform conducts by ≈ 2 orders of magnitude better than a corresponding vacuum gap (see black and yellow curves). At $z = 2.4$ Å, the conductance (black) abruptly rises. Since the Au apex atom is approaching the reactive center of the platform, a similar mechanism like for the pure Au contact may be expected and we attribute the abrupt rise to the formation of a Au–C bond between the tip and the molecule. The related conductance after contact formation (black dashed horizontal line), $\approx 3.5 \times 10^{-1}$ G_0, is high compared to other molecules connected to Au electrodes [33–35] and close to that of a pure Au point contact (≈ 1 G_0). However, a bond to a functional group may drastically change the electronic structure of the platform and may reduce the conductance.

For a given z, the moieties attached to the TOTA platform (figures 1(a)–(d)) reduce the distance between the tip and the molecules. Naively a corresponding conductance increase would be expected in the tunneling regime. However, the conductance of H-TOTA (cyan curve) at large separations ($z > 5$ Å) is ≈ 4 times lower than that of the bare platform (black, figure 1(i)). In addition, the conductance of Me-TOTA (red curve) is about as large as that of TOTA (black). This effect is caused by substantial electronic differences between
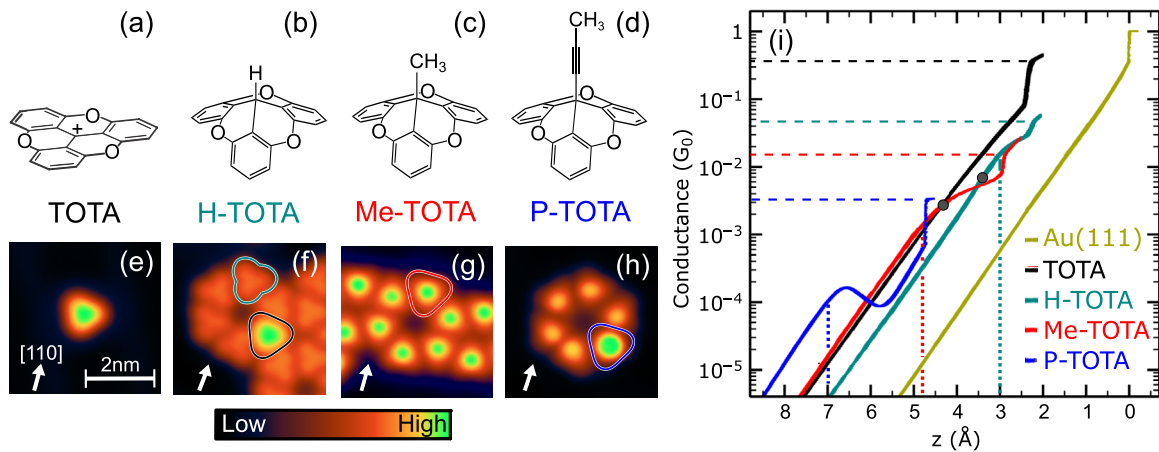
Figure 1. (a)–(d) Lewis structures of trioxatriangulenium (TOTA), H-TOTA, Me-TOTA, and P-TOTA. The lengths of the functional groups measured from the central C atom of the platform to the topmost H atoms are 1.1, 2.0, and 4.5 Å (from left to right). (e)–(h) Constant-current STM topographs of (e) a single TOTA, (f) a cluster of H-TOTA (cyan) along with a single TOTA (black), (g) a cluster of Me-TOTA (red) and (h) a single P-TOTA (blue) embedded in a cluster of 5 Ethyl-TOTA molecules ($V = 100$ mV, $I = 30$ pA). The apparent heights of the molecules (a)–(d) in these images are 2.2, 1.6, 2.3, and 3.2 Å, respectively. White arrows indicate a $\langle 1\,1\,1 \rangle$ direction of the Au lattice. (i) Experimental conductance curves $G(z)$ of TOTA (black), H-TOTA (cyan), Me-TOTA (red) and P-TOTA (blue) in units of the quantum of conductance $G_0 \doteq 2e^2/h$ (e: elementary charge, h: Planck constant). Zero tip position is defined as contact of the Au tip to a fcc area of the Au(1 1 1) substrate (yellow). The conductance curves of the molecules consists of at least 10 forward and 10 backward traces.

TOTA and the functionalized platforms. TOTA on Au(1 1 1) has its lowest unoccupied molecular orbital (LUMO) at $\approx E_F + 0.6$ eV, while states of the functionalized platforms that protrude towards the tip are located at energies below $E_F - 1.5$ eV, much farther away from E_F (see supporting information (SI) (stacks.iop.org/JPhysCM/31/18LT01/mmedia), section I). As a result, these states contribute less to the current than the LUMO of the bare platform.

For $G \lesssim 10^{-4}\, G_0$, the sequence of the conductances of the functionalized platforms reflects the lengths of the attached moieties. Surprisingly all molecules studied here exhibit a similar apparent tunneling barrier height of ≈ 4 eV.

At smaller separations, intriguing deviations from an exponential conductance evolution occur (figure 1(i), dotted vertical lines) suggesting that forces between the molecule and the tip are involved. The slope of the conductance of Me-TOTA (red) begins to reduce at $z \approx 4.8$ Å ($G \approx 1.5 \times 10^{-3}\, G_0$) indicating that mechanical contact occurs (red dotted vertical line). Mechanical contact to H-TOTA (cyan) sets in at $z = 3$ Å (cyan dotted vertical line), i.e. 1.8 Å closer to the surface compared to Me-TOTA. This value may be caused by (i) the position of the topmost H atom (0.9 Å lower in H-TOTA) and (ii) a smaller tip-induced force acting on the H atom than on a methyl moiety. In the case of P-TOTA (blue curve), the change of slope begins at $z \approx 7$ Å (blue dotted vertical line) and $G \approx 10^{-4}\, G_0$. Taking into account that P-TOTA has an extra ethynyl spacer compared to Me-TOTA (length ≈ 2.5 Å), we find that mechanical interaction starts at similar tip-methyl distances (distance of the blue and the red dotted vertical line ≈ 2.2 Å).

The conductances of Me-TOTA (red) and P-TOTA (blue, figure 1(i)) at the onset of mechanical contact differ by one order of magnitude. Compared to Me-TOTA, the current path through P-TOTA is longer by ≈ 2.5 Å. In vacuum, this increase of the path length would reduce the conductance by

a factor of ≈ 100. Hence, the ethynyl unit is one order of magnitude more conductive than a vacuum gap of the same size.

As discussed in [22], the complex conductance variation of P-TOTA results from short range repulsion between the topmost methyl moiety (figure 1(d)) and the tip apex. The propynyl wire bends while the tip-molecule and the molecule-substrate separations remain almost constant. The deformation induces a symmetry mismatch of the current-carrying orbitals at the tip-molecule interface that drastically reduces the conductance. As a result, at $z \approx 5.8$ Å, P-TOTA (blue) is ≈ 2.5 less conductive than Me-TOTA (red). In the range $z \approx 5.8$ to ≈ 4.8 Å the conductance G rises exponentially because the distance of the tip apex atom and the C atoms of the propynyl moiety, that are originally triple bonded (figure 1(d)), is reduced. The steep rise of G at ≈ 4.8 Å is due to bond formation between these C atoms and the apex atom [22]. Such bonding of Au clusters or cationic Au atoms to triple-bonded C atoms (Au–C–C bond) is well studied [36–38], partially because it represents the highly important activation step of C≡C triple bonds towards nucleophiles in a catalytic cycle. The related strong hybridization of a LUMO of P-TOTA leads to new tip-molecule states close to E_F that dominate the current flow.

During contact formation to Me-TOTA and H-TOTA the formation of a chemical bond is *not* expected, because the reactive center of TOTA is passivated by inert and rigid functional groups like a H atom or a methyl moiety[5]. Nevertheless, we observe abrupt increases of the conductance at positions $z = 2.3$ Å and 3 Å for H-TOTA (cyan) and Me-TOTA (red curve), respectively. The corresponding conductances of ≈ 1–$5 \times 10^{-2}\, G_0$ are relatively high. For example, non-bonding Xe–Xe and CO-C_2H_2 contacts were reported to exhibit conductances that are an order of magnitude lower [28, 39]. Considering the approximate sizes of H (1.1 Å) and methyl (2.0 Å) and the fact that bond formation to the bare platform
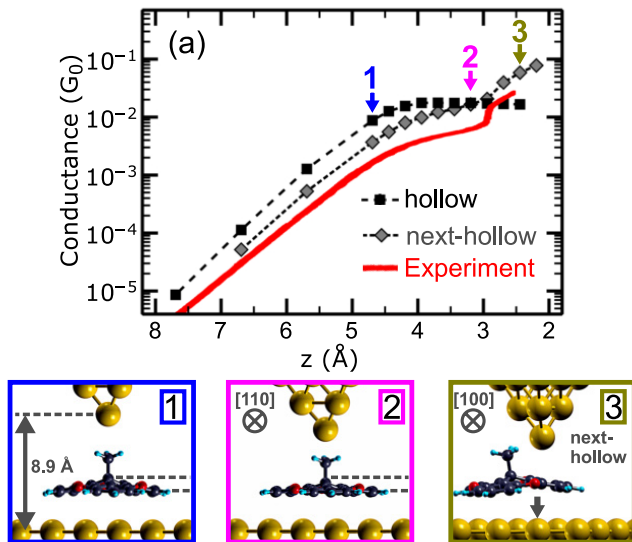
Figure 2. (a) Theoretical and experimental conductance curves $G(z)$ of Me-TOTA. In the experiment (red), the tip was centered above the molecule before bringing it closer. Calculated conductances for the molecule located at a hollow (an adjacent hollow site) with the tip centered above the hollow site are shown by black squares (gray diamonds). The value $z = 0$ Å refers to the distance where a jump to contact is observed (see yellow curve in figure 1(i)). It corresponds to a distance of 4.3 Å between the bare surface and the apex of a frozen tip. (**1–3**) Calculated junction geometries corresponding to $z = 4.7$, 3.2 and 2.4 Å as indicated in panel (a). In configurations **1** and **2** (configuration **3**) the molecule is placed at the hollow (next-hollow) site. **1** and **2** are shown as side views in a $\langle 1\,1\,0 \rangle$ direction. **3** is viewed from a $\langle 100 \rangle$ direction. The arrow in **3** indicates the positon of the hollow site.

Figure 3. Calculated results for Me-TOTA at a hollow site with the tip centered above the molecule. (a) Energy change of the subsystems tip-molecule (black squares), molecule (grey circles), and tip (yellow diamonds) versus z. The energy of each subsystem was calculated as the total energy of a junction from which all atoms that are not part of the subsystem are removed while keeping all other atomic positions fixed. Arrows indicate results for configurations **1** and **2** from figure 2. (b) Definition of distances. d_1: from outer C atoms of the platform to surface. d_2: from central C atom of the platform to surface. d_3: from apex atom to C atom of the methyl moiety. (c) Geometry changes of the metal-molecule interfaces versus z. Results for distances d_1, d_2, and d_3 are indicated by black squares, grey circles, and yellow crosses, respectively. In the calculations a tetrahedral tip comprised of 3 Au(1 1 1) layers was used. Its length d_4 is defined as the distance of the apex atom to a reference plane at the base of the tip. (d) Energy change versus rigid displacement Δd_1 (see pictogram) for junction configurations corresponding to $z = 7.7$ (black), 4.7 (blue), 3.2 (magenta) and 2.4 Å (yellow). $\Delta d_1 > 0$ indicates displacements of Me-TOTA towards the tip. A Morse potential fit to the black data points is shown by a black solid line.

occurs at $z = 2.5$ Å, drastic changes of the conductance are *expected* to occur at z values that are much larger (gray circles in figure 1(i)). The surprisingly low z values of the abrupt increases suggest that significant geometric changes of the junctions are involved. In order to understand the intriguing variations of the conductance of H-TOTA and Me-TOTA, we henceforth focus on the Me-TOTA junction. Most likely, the results are transferable to the H-TOTA junction.

Theoretical results

Conductance and tip-induced geometry changes

The transport properties of Me-TOTA in a STM junction were calculated using density functional theory (DFT) combined with nonequilibrium Green's function (NEGF) methods (see Methods). Figure 2(a) displays the calculated zero-bias conductance (black and grey) along with the experimental data (red) versus electrode separation z.

For large tip-molecule separations the DFT calculations favor a Me-TOTA position at a hollow site of the substrate (see SI, section II). The tip is centered above the molecule as in configuration **1** of figure 2. When the electrode separation is smaller than in configuration **1**, repulsive interaction between the methyl moiety and the tip occurs. At $z = 3.2$ and 3.0 Å the adjacent hollow sites (next-hollow) are already 0.35 eV and 0.50 eV more favorable than the initial hollow site (see SI,
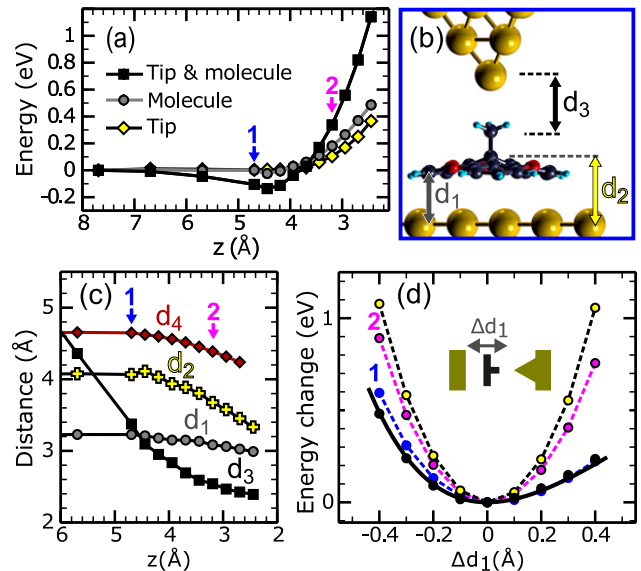
section II). Consequently, instead of adopting configuration **2**, Me-TOTA shifts to an adjacent hollow site to relax strain. Configuration **3** displays the resulting geometry at small electrode separation ($z = 2.4$ Å).

The conductance calculated for the molecule and the tip centered on a hollow site (configurations **1** and **2**) is shown by black squares. It reproduces the experimental trend (neglecting an overestimation by a factor of ≈ 4, which is typical of DFT+NEGF results because DFT tends to underestimate HOMO–LUMO gaps [40]) but saturates for $z \lesssim 4$ Å in contrast to the experimental observations. The conductance for an adjacent hollow position of the molecule with the tip still centered over the original hollow site (configuration **3**) is displayed by gray diamonds. It exhibits a further rise of G as observed in the experiments. We therefore attribute the $G(z)$ data and, in particular, the rapid rise at $z \approx 3$ Å to a reversible lateral shift of the molecule from its original hollow position to an adjacent hollow site. The experimentally probed molecules are embedded into molecular clusters. These clusters are too large to model them on the level of calculation we used. In our simplified model with only a single molecule, for

large tip-molecule separations, neighboring adsorption sites have approximately the same energy (see SI, figure S2). The displacement of single molecules is therefore not expected to be reversible and a hysteresis may occur. However, in the experiments intermolecular forces within a cluster usually prevent hysteresis (see figure 1(i)). The interpretation that Me-TOTA reversibly laterally shifts is also consistent with the observation that irreversible changes of the conductance only occurred for $z \lesssim 3$ Å and changed the arrangement of Me-TOTA in clusters. A related scenario of reversible hopping between adjacent hollow sites was previously reported for single Co and Ag atoms on Cu(1 1 1) and Ag(1 1 1), respectively [41, 42]. In that case, local heating and attractive forces of the tip lead to bistability. Here, we emphasize that the abrupt conductance variation of Me-TOTA does not involve chemical bond formation.

Mechanical coupling at the metal-molecule interface

To analyze the mechanical properties of the junctions we determined the energy of the tip-molecule subsystem (figure 3(a), black squares), which we define as the total energy of a junction from which all substrate atoms are removed while keeping the positions of the remaining atoms fixed. This energy is not affected by changes of the molecule-substrate interface. For Me-TOTA and different electrode separations with the tip centered above the molecule a shallow minimum of -140 meV (figure 3(a), black squares) occurs close to configuration **1** of figure 2 confirming that no covalent or other chemical bond (binding energy $\gtrsim 0.5$ eV) between the tip and the molecule is formed. The absence of a chemical bond is also obvious from only marginal redistribution of electron charge within the molecule and the tip (see SI, section III). In the repulsive regime ($z \lesssim 4$ Å), the tip-molecule energy (black squares) drastically increases as expected. Moreover, the repulsion of the tip and the methyl moiety induces a rapid increase of the strain energies of the molecule (gray circles) and the tip (yellow diamonds).

Although the tip presses on the molecule, the distance d_1 between the platform and the surface hardly changes (<0.2 Å) when the tip is moved 1.8 Å towards the molecule (figures 3(b) and (c)). The platform is, however, flattened as indicated by the decreasing height of the central C atom of the platform (d_2 of figures 3(b) and (c)). Moreover, the tip is compressed (d_4 in figure 3(c)). These deformations prevent the tip apex from approaching the methyl group (d_3 in figures 3(b) and (c)). Consequently, the geometry of the tip-molecule and molecule-surface interfaces change only little compared to that of the molecule and the tip. Thus, both interfaces turn out to be more rigid than the molecule (figure 3(a), gray circles) and the tip (figure 3(a), yellow diamonds). This comes as a surprise, because the molecule is physisorbed.

To quantify the stiffness of the interfaces we calculated the energy change of the junction upon a rigid vertical displacement of the molecule (figure 3(d)). When the influence of the tip is negligible (black and blue circles), the molecule-surface interaction can be modeled by an effective Morse potential (black curve). For the fit (black curve) the potential depth was set to the calculated adsorption energy of 1.8 eV. A force constant of 7 nN Å^{-1} is extracted from the fit. This value is comparable to those reported for covalent S–Au bonds (S–Au(1 1 1): 7–10 nN Å^{-1} [43] or S–Au$^+$: 17 nN Å^{-1} [44]) and also matches results for C$_{60}$ on Au electrodes [45]. The binding energies of a S atom (up to 1.8 eV [46, 47]) and the TOTA platform are similar as well. These results show that physisorption of an extended π system to a metal provides stable adsorption heights and thus is an attractive alternative to other bonding schemes.

Deeper in the repulsive regime ($z \lesssim 3.5$ Å, magenta and yellow circles in figure 3(d)) the energies for lifting and lowering the molecule become similar. The symmetry of the parabolas shows that the molecule is much deformed and thus rigidly couples the tip and the substrate.

The electrode-molecule interfaces may be viewed as hard springs (figure 3(d)), while the molecule itself and the STM tip are more compliant (gray circles and yellow diamonds of figure 3(a)). In a lateral direction, however, the stability of the position of the platform is low. Strain is therefore relaxed by the aforementioned lateral shift.

Impact of the electrodes on the molecular orbitals

As molecular orbitals lead to resonances of the electron transmission through the junctions, changes of the molecular orbitals may control the conductance during contact formation. Therefore, we calculated the influence of the tip-molecule and surface-molecule interactions on the molecular orbitals via the molecular projected self-consistent Hamiltonian (MPSH) [48, 49]. For a molecule at a hollow position (figures 4(a)–(f)) the spatial shapes of the MPSH states are hardly affected by the tip position and correspond to the molecular states of the gas-phase molecule. Surface-molecule and tip-molecule interactions are fairly unimportant in this case. For a molecule at an adjacent hollow position and at small electrode separation (figures 4(g)–(i)) the interaction with the tip leads to a slight increase of the MPSH density between the tip and the molecule. We attribute this effect to the electrostatic interaction of the tip and the molecule, which does not crucially affect the transmission through the states (see SI, section IV). In addition to the orbitals' shapes, the energy separations of the orbitals close to E_F are hardly affected by the interaction with the surface and the tip (figures 4(a)–(i) and SI, section IV). For example, the resulting gaps between the HOMO (highest occupied molecular orbital) and LUMO of Me-TOTA for configurations **2** (3.63 eV) and **3** (3.67 eV) from figure 2 are almost identical to the calculated gas-phase value (3.73 eV). Accordingly the conductance is *not* controlled by significant changes of the current-carrying orbitals. Instead, it is closely related to the geometry of the tip-molecule-surface junction.
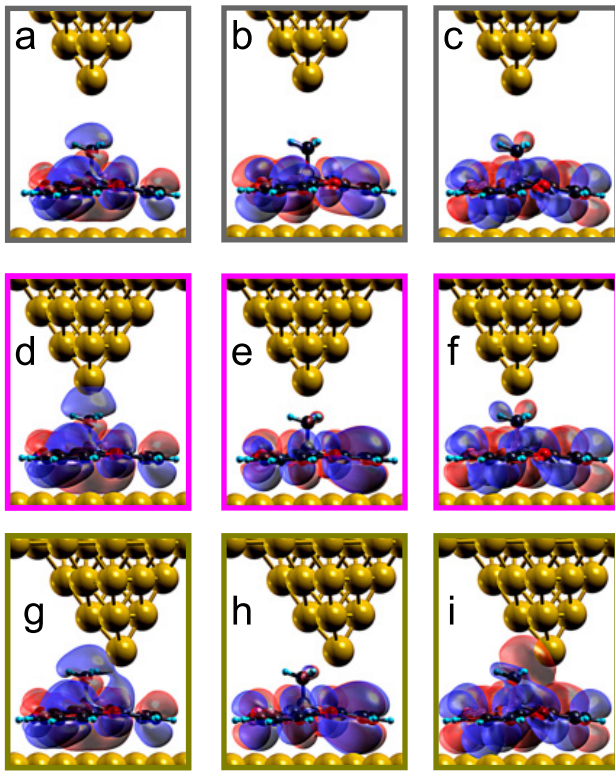
Figure 4. (a)–(i) Isosurfaces of the HOMO-1, HOMO, and LUMO (left to right) of the MPSH Hamiltonian for different configurations. Blue and red colors indicate the sign of the wave functions. The HOMO and LUMO are both degenerate or nearly degenerate. As the shapes of the degenerate states are similar, only one of them is shown. (a)–(c) $z = 5.7$ Å with eigenenergies at $E − E_F = −1.56$, $−1.14$, and $2.54\,eV$ (left to right), (d)–(f) $z = 3.2$ Å (configuration **2**) with eigenenergies at $−1.83$, $−1.43$, and $2.20\,eV$, (g)–(i) $z = 2.7$ Å (close to configuration **3**) with eigenenergies at $−1.72$, $−1.33$, and $2.35\,eV$.

Electron transport mechanisms

At electrode separations larger than in configuration **1** of figure 2, the vacuum gap represents the bottleneck for electron transmission. In configuration **1**, however, the bottleneck has shifted to the molecule-substrate interface as revealed by the calculated eigenchannel (figure 5(a)). As seen, the scattering state on the molecule reflects the HOMO-1 (see figure 5(e)), which dominates the transmission at E_F (see SI, section IV). The HOMO (figure 5(f)) is $\approx 0.5\,eV$ closer to E_F than the HOMO-1 (figure 5(e)) but hardly contributes to the conductance because of its orbital symmetry. The local symmetry of the HOMO-1 at the methyl group is *s*-like, matches the tip *s* wave (figure 5(a)), and provides large overlap and good electrical contact. By contrast, the HOMO exhibits a *p*-like shape at the methyl moiety. Its nodal plane reduces the overlap with the tip and leads to a bad electrical contact. The LUMO is farther away from E_F and only has a weak impact on the conductance.

A projection of the transmission onto either all occupied or all empty states of the MPSH Hamiltonian (see SI, section IV) reveals that transport pathways through the empty states of Me-TOTA near E_F interfere *destructively* with those through the occupied states. For P-TOTA we find the opposite effect,
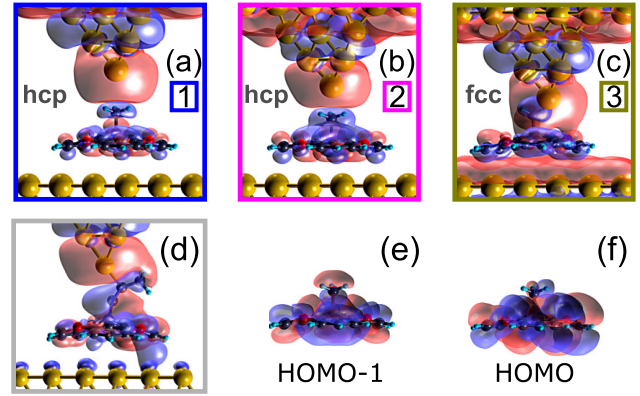

Figure 5. (a)–(c) Isosurface plots of the real part of the most transmitting eigenchannels of configurations **1**–**3** of Me-TOTA (side views in the $[1\,1\,0]$ direction). Electron waves coming in from the tip electrode at the $\bar{\Gamma}$ point. (d) Isosurface plot for P-TOTA at $z = 4.8$ Å. (e) and (f) isosurface plots of the HOMO-1 and the HOMO of Me-TOTA in the gas phase.

i.e. the occupied and empty states interfere *constructively* (see SI, section IV). This shows that a functional group can change the interference properties of a molecular bridge, as previously reported, e.g. for anthracene and anthraquinone based molecular wires [50].

Between configurations **1** and **2** the conductance varies weakly (figure 2). While the molecule-substrate distance and the molecular states (see above) hardly change, the distance between the tip and the molecule shrinks despite the tip-induced deformation of the molecule. The lack of a corresponding increase of the conductance indicates that the coupling of the tip and the methyl group is almost saturated in configuration **1**. This is confirmed by the scattering states that hardly change from configuration **1** to **2** (figures 5(a) and (b)).

As shown above, to relax the repulsive forces across the junction, Me-TOTA shifts to an adjacent hollow position like in configuration **3** of figure 2. The shift affects the current in two ways (figure 5(c)). First, the coupling of the tip *s* wave and the methyl moiety changes, because the nodal plane of the HOMO is no longer located at the tip position. Second, the vacuum-tunneling gap between the tip and the platform itself closes for small tip-molecule distances. As a result, the scattering state of configuration **3** exhibits no localized transmission bottleneck and the conductance increases but still remains $< 0.1\,G_0$.

Remarkably, the geometries of the current paths through Me-TOTA and P-TOTA, namely a single C atom protruding from the platform, are similar around $z = 4.8$ Å (see figures 5(a) and (d)). In the case of Me-TOTA, a soft mechanical contact with weak attractive interaction is formed, whereas P-TOTA covalently binds to the tip. Despite this difference the conductances differ only by a factor of 2. At further reduced electrode separations ($z \approx 3.8$ Å) the mechanical contact actually conducts better ($\approx 35\%$) and is still slightly attractive (figure 3(a)).

Chemical bonding changes the electronic structure of the electrodes-molecule junction and in particular the electronic structure of the molecule. Avoiding this complexity, i.e.

preserving the electronic structure of the molecule despite attachment to an electrode, may simplify the design of a molecule with specific transport properties [2, 3, 8–10, 17].

Conclusions

We synthesized molecules that physisorb on a metal substrate with a wide platform and make a functional unit stand vertically. Conductance data from low-temperature STM contacts exhibit little scatter and show that the π system of the platform provides a good electrical and mechanical contact to the substrate. This makes possible a detailed comparison between functional groups that are inert (methyl, H) or bind (propynyl, bare TOTA platform) to the tip. The lengths of the functional groups are reflected by the range of tip-molecule distances where deviations from an exponential conductance variation occur. All molecules exhibit a rapid conductance rise at small separations. The reasons under lying the rise in the cases of inert and binding subunits, however, are widely different, namely lateral motion versus bond formation. The conductance of methyl TOTA at contact formation is only twice that of propynyl TOTA, which differs from methyl by an ethynyl spacer. Yet, similar conductances arise because the spacer is circumvented by the tip and because different orbitals carry the current. The results show that the platform anchor group and pm-control of the electrode position lead to reproducible contacts and large conductance without requiring chemisorption. Despite the simplicity of the functional groups used the conductance evolutions have multifaceted origins.

Methods

Experimental details. Measurements were performed with a STM operated at 4.6 K and in ultrahigh vacuum (base pressure 10^{-9} Pa). Au(1 1 1) surfaces and chemically etched W tips were cleaned by repeated Ar$^+$ bombardment and annealing. After mounting into the STM, the tips were repeatedly indented into the substrate. To obtain a sharp tip the sample was repeatedly contacted with the tip until the contacts were stable at a conductance $G \approx G_0$ (see yellow curve in figure 1(i)) and adatoms were imaged as circular protrusions of <700 pm diameter. This indicates that the tip apex is comprised of a single Au atom. As a result, the contacted molecules are essentially probed by an *s* wave close to E_{F}. We verified that tips were not modified during measurements on molecules via STM imaging.

Functionalized molecules were sublimated onto Au(1 1 1) at ambient temperature from a heated Ta crucible at pressures $\lesssim 10^{-8}$ Pa. Details of the syntheses can be found in [22, 51–53].

Computational methods. Simulations were performed with SIESTA [54] and TRANSIESTA [49, 55] taking into account dispersion interactions [56]. The supercell contains a single Me-TOTA molecule adsorbed on a 10-layer Au(1 1 1) slab with 6×6 periodicity. A 10-atom Au(1 1 1) tetrahedron, mounted on the reverse side of the slab, represents the STM tip apex.

We used a double-ζ plus polarization basis set with 0.02 eV energy shift for C, H, and O, as well as for the Au tip and surface layer atoms. For the bulk Au atoms, we used a single-ζ plus polarization basis with 0.02 Ry (0.272 eV) energy shift. Atomic coordinates of molecule, tip, and surface layer were relaxed until forces were smaller than 0.04 eV Å^{-1}. A cutoff of 400 Ry was used for the real-space grid integrations. The electronic structure was computed on a $2 \times 2 \times 1$ Monkhorst–Pack *k*-mesh. The transmission functions were sampled over 21×21 *k*-points. Projection of transmissions onto MPHS states were performed as described in [49]. Eigenchannel scattering states were computed with INELASTICA [57–59].

ORCID iDs

Torben Jasper-Tönnies https://orcid.org/0000-0001-5087-3959
Aran Garcia-Lekue https://orcid.org/0000-0001-5556-0898
Thomas Frederiksen https://orcid.org/0000-0001-7523-7641
Rainer Herges https://orcid.org/0000-0002-6396-6991
Richard Berndt https://orcid.org/0000-0003-1165-9065

References

[1] Nitzan A and Ratner M A 2003 Electron transport in molecular wire junctions *Science* **300** 1385
[2] Tao N J 2006 Electron transport in molecular junctions *Nat. Nanotechnol.* **1** 173–81
[3] Chen F, Hihath J, Huang Z, Li X and Tao N 2007 Measurement of single-molecule conductance *Annu. Rev. Phys. Chem.* **58** 535–64
[4] Kiguchi M and Kaneko S 2012 Electron transport through single π-conjugated molecules bridging between metal electrodes *ChemPhysChem* **13** 1116–26
[5] Leary E, Rosa A L, González M T, Rubio-Bollinger G, Agraït N and Martín N 2015 Incorporating single molecules into electrical circuits. The role of the chemical anchoring group *Chem. Soc. Rev.* **44** 920–42
[6] Esat T, Friedrich N, Tautz F S and Temirov R 2018 A standing molecule as a single-electron field emitter *Nature* **558** 573–6
[7] Reuter M G, Seideman T and Ratner M A 2011 Guidelines for choosing molecular 'alligator clip' binding motifs in electron transport devices *J. Chem. Phys.* **134** 154708
[8] Moth-Poulsen K and Bjørnholm T 2009 Molecular electronics with single molecules in solid-state devices *Nat. Nanotechnol.* **4** 551–6
[9] von Wrochem F, Gao D, Scholz F, Nothofer H-G, Nelles G and Wessels J M 2010 Efficient electronic coupling and improved stability with dithiocarbamate-based molecular junctions *Nat. Nanotechnol.* **5** 618–24
[10] Wang Y F, Kröger J, Berndt R, Vázquez H, Brandbyge M and Paulsson M 2010 Atomic-scale control of electron transport through single molecules *Phys. Rev. Lett.* **104** 176802

[11] Altenburg S J, Kröger J, Wang B, Bocquet M-L, Lorente N and Berndt R 2010 Graphene on Ru(0 0 0 1): contact formation and chemical reactivity on the atomic scale *Phys. Rev. Lett.* **105** 236101

[12] Kiguchi M and Kaneko S 2013 Single molecule bridging between metal electrodes *Phys. Chem. Chem. Phys.* **15** 2253–67

[13] Frederiksen T, Foti G, Scheurer F, Speisser V and Schull G 2014 Chemical control of electrical contact to sp^2 carbon atoms *Nat. Commun.* **5** 4659

[14] Zhang Y, Wang Y, Lü J-T, Brandbyge M and Berndt R 2017 Mechanochemistry induced using force exerted by a functionalized microscope tip *Angew. Chem.* **129** 11931–5

[15] Karan S, García C, Karolak M, Jacob D, Lorente N and Berndt R 2017 Spin control induced by molecular charging in a transport junction *Nano Lett.* **18** 88–93

[16] Sun L, Diaz-Fernandez Y A, Gschneidtner T A, Westerlund F, Lara-Avila S and Moth-Poulsen K 2014 Single-molecule electronics: from chemical design to functional devices *Chem. Soc. Rev.* **43** 7378–411

[17] Kaliginedi V, Rudnev A V, Moreno-Garcia P, Baghernejad M, Huang C, Hong W and Wandlowski T 2014 Promising anchoring groups for single-molecule conductance measurements *Phys. Chem. Chem. Phys.* **16** 23529

[18] Valášek M and Mayor M 2017 Spatial and lateral control of functionality by rigid molecular platforms *Chem. Eur. J.* **23** 13538–48

[19] Baisch B, Raffa D, Jung U, Magnussen O M, Nicolas C, Lacour J, Kubitschke J and Herges R 2009 Mounting freestanding molecular functions onto surfaces: the platform approach *J. Am. Chem. Soc.* **131** 442–3

[20] Wei Z *et al* 2014 Triazatriangulene as binding group for molecular electronics *Langmuir* **30** 14868–76

[21] Hauptmann N, Groß L, Buchmann K, Scheil K, Schütt C, Otte F L, Herges R, Herrmann C and Berndt R 2015 High-conductance surface-anchoring of a mechanically flexible platform-based porphyrin complex *New J. Phys.* **17** 013012

[22] Jasper-Tönnies T, Garcia-Lekue A, Frederiksen T, Ulrich S, Herges R and Berndt R 2017 Conductance of a freestanding conjugated molecular wire *Phys. Rev. Lett.* **119** 066801

[23] Yelin T, Korytár R, Sukenik N, Vardimon R, Kumar B, Nuckolls C, Evers F and Tal O 2016 Conductance saturation in a series of highly transmitting molecular junctions *Nat. Mater.* **15** 444–9

[24] Martin C A, Ding D, Sørensen J K, Bjørnholm T, van Ruitenbeek J M and van der Zant H S J 2008 Fullerene-based anchoring groups for molecular electronics *J. Am. Chem. Soc.* **130** 13198–9

[25] Leary E, González M T, van der Pol C, Bryce M R, Filippone S, Martín N, Rubio-Bollinger G and Agraït N 2011 Unambiguous one-molecule conductance measurements under ambient conditions *Nano Lett.* **11** 2236–41

[26] Bader R F W 2003 *Atoms in Molecules, Handbook of Molecular Physics and Quantum Chemistry* vol **2** (Chicester: Wiley)

[27] Chen C J 1990 Tunneling matrix elements in three-dimensional space: the derivative rule and the sum rule *Phys. Rev.* B **42** 8841–57

[28] Corso M, Ondráček M, Lotze C, Hapala P, Franke K J, Jelínek P and Pascual J I 2015 Charge redistribution and transport in molecular contacts *Phys. Rev. Lett.* **115** 136101

[29] Liljeroth P, Repp J and Meyer G 2007 Current-induced hydrogen tautomerization and conductance switching of naphthalocyanine molecules *Science* **317** 1203–6

[30] Pan S, Fu Q, Huang T, Zhao A, Wang B, Luo Y, Yang J and Hou J 2009 Design and control of electron transport properties of single molecules *Proc. Natl Acad. Sci. USA* **106** 15259–63

[31] Landman U, Luedtke W D, Burnham N A and Colton R J 1990 Atomistic mechanisms and dynamics of adhesion, nanoindentation, and fracture *Science* **248** 454–61

[32] Olesen L, Brandbyge M, Sørensen M R, Jacobsen K W, Lægsgaard E, Stensgaard I and Besenbacher F 1996 Apparent barrier height in scanning tunneling microscopy revisited *Phys. Rev. Lett.* **76** 1485–8

[33] Komoto Y, Fujii S, Iwane M and Kiguchi M 2016 Single-molecule junctions for molecular electronics *J. Mater. Chem.* C **4** 8842–58

[34] Zang Y, Pinkard A, Liu Z-F, Neaton J B, Steigerwald M L, Roy X and Venkataraman L 2017 Electronically transparent Au–N bonds for molecular junctions *J. Am. Chem. Soc.* **139** 14845–8

[35] Carini M, Ruiz M P, Usabiaga I, Fernández J A, Cocinero E J, Melle-Franco M, Diez-Perez I and Mateo-Alonso A 2017 High conductance values in π-folded molecular junctions *Nat. Commun.* **8** 15195

[36] Wang Y, Zhu M, Kang L and Dai B 2014 Neutral Aun($n = 3$–10) clusters catalyze acetylene hydrochlorination: a density functional theory study *RSC Adv.* **4** 38466

[37] Ferraro F, Pérez-Torres J F and Hadad C 2015 Selective catalytic activation of acetylene by a neutral gold cluster of experimentally known gas-phase geometry *J. Phys. Chem.* C **119** 7755–64

[38] Bistoni G, Belanzoni P, Belpassi L and Tarantelli F 2016 π Activation of alkynes in homogeneous and heterogeneous gold catalysis *J. Phys. Chem.* A **120** 5239–47

[39] Yazdani A, Eigler D M and Lang N D 1996 Off-resonance conduction through atomic wires *Science* **272** 1921–4

[40] Godby R W, Schlüter M and Sham L J 1986 Accurate exchange-correlation potential for silicon and its discontinuity on addition of an electron *Phys. Rev. Lett.* **56** 2415–8

[41] Stroscio J A and Celotta R J 2004 *Science* **306** 242

[42] Sperl A, Kröger J and Berndt R 2010 Direct observation of conductance fluctuations of a single-atom tunneling contact *Phys. Rev.* B **81** 035406

[43] Sellers H, Ulman A, Shnidman Y and Eilers J E 1993 Structure and binding of alkanethiolates on gold and silver surfaces: implications for self-assembled monolayers *J. Am. Chem. Soc.* **115** 9389–401

[44] Butler I S, Neppel A, Plowman K R and Shaw C F 1984 Vibrational spectra and normal coordinate calculations for some dimethyl sulfide complexes of gold(I) and gold(III) *J. Raman Spectrosc.* **15** 310–8

[45] Park H, Park J, Lim A K L, Anderson E H, Alivisatos A P and McEuen P L 2000 Nanomechanical oscillations in a single-C_{60} transistor *Nature* **407** 57–60

[46] Schwarz F and Lörtscher E 2014 Break-junctions for investigating transport at the molecular scale *J. Phys.: Condens. Matter* **26** 474201

[47] Franke A and Pehlke E 2009 Adsorption and diffusion of SCH$_3$ radicals and Au(SCH$_3$)$_2$ complexes on the unreconstructed Au(1 1 1) surface in the submonolayer coverage regime *Phys. Rev.* B **79** 235441

[48] Stokbro K, Taylor J, Brandbyge M, Mozos J-L and Ordejon P 2003 Theoretical study of the nonlinear conductance of Di-thiol benzene coupled to Au(1 1 1) surfaces via thiol and thiolate bonds *Comput. Mater. Sci.* **27** 151–60

[49] Papior N, Lorente N, Frederiksen T, García A and Brandbyge M 2017 Improvements on non-equilibrium and transport Green function techniques: the next-generation transiesta *Comput. Phys. Comm.* **212** 8–24

[50] Guédon C M, Valkenier H, Markussen T, Thygesen K S, Hummelen J C and van der Molen S J 2012 Observation of quantum interference in molecular charge transport *Nat. Nanotechnol.* **7** 305–9

[51] Martin J C and Smith R G 1964 Factors influencing the basicities of triarylcarbinols. The synthesis of sesquixanthydrol *J. Am. Chem. Soc.* **86** 2252–6

[52] Lofthagen M, VernonClark R, Baldridge K K and Siegel J S 1992 Synthesis of trioxatricornan and derivatives. Useful keystones for the construction of rigid molecular cavities *J. Org. Chem.* **57** 61–9

[53] Faldt A, Krebs F C and Thorup N 1997 Synthesis, structure and properties of various molecules based on the 4,8,12-trioxa-4,8,12,12c-tetrahydrodibenzo[*cdmn*]pyrene system with an evaluation of the effect differing molecular substituti on patterns has on the space group symmetry *J. Chem. Soc. Perkin Trans.* **20** 2219–28

[54] Soler J M, Artacho E, Gale J D, Garía A, Junquera J, Ordejón P and Sánchez-Portal D 2002 The SIESTA method for *ab initio* orden-N materials simulation *J. Phys.: Condens. Matter* **11** 2745–79

[55] Brandbyge M, Mozos J L, Ordejón P, Taylor J and Stokbro K 2002 Density-functional method for nonequilibrium electron transport *Phys. Rev.* B **65** 165401

[56] Klimeš J, Bowler D R and Michaelides A 2010 Chemical accuracy for the van der Waals density functional *J. Phys.: Condens. Matter* **22** 022201

[57] Paulsson M and Brandbyge M 2007 Transmission eigenchannels from nonequilibrium Green's functions *Phys. Rev.* B **76** 115117

[58] Frederiksen T, Paulsson M, Brandbyge M and Jauho A-P 2007 Inelastic transport theory from first principles: methodology and application to nanoscale devices *Phys. Rev.* B **75** 205413

[59] Inelastica software suite https://github.com/tfrederiksen/inelastica/